



Lewandowska, AE., & Eichhorn, SJ. (2016). Quantification of the degree of mixing of cellulose nanocrystals in thermoplastics using Raman spectroscopy. *Journal of Raman Spectroscopy*, 47(11), 1337-1342. <https://doi.org/10.1002/jrs.4966>

Peer reviewed version

Link to published version (if available):  
[10.1002/jrs.4966](https://doi.org/10.1002/jrs.4966)

[Link to publication record in Explore Bristol Research](#)  
PDF-document

This is the author accepted manuscript (AAM). The final published version (version of record) is available online via WILEY at <https://onlinelibrary.wiley.com/doi/abs/10.1002/jrs.4966>. Please refer to any applicable terms of use of the publisher.

## University of Bristol - Explore Bristol Research

### General rights

This document is made available in accordance with publisher policies. Please cite only the published version using the reference above. Full terms of use are available:  
<http://www.bristol.ac.uk/red/research-policy/pure/user-guides/ebr-terms/>

# Quantification of the degree of mixing of cellulose nanocrystals in thermoplastics using Raman spectroscopy

A.E. Lewandowska, S.J. Eichhorn\*

College of Engineering, Maths & Physical Sciences, University of Exeter, Physics Building, Stocker Road, Exeter, EX4 4QL, UK.

## Abstract

A combination of Raman imaging with image analysis has been used to quantify the degree of mixing of cellulose nanocrystals (CNCs) in melt compounded high density polyethylene (HDPE). Raman spectroscopy is shown to provide an accurate “fingerprint” of the composition of the cross-sectional area of the end section of a formed composite. This information is then converted to a chemical image allowing spatial quantification of the mixing of CNCs in the HDPE. A degree of mixing between CNCs and HDPE is reported, with a strong tendency for the former to agglomerate with little dispersion. Freeze-dried CNCs show better mixing with HDPE and a lower tendency to agglomerate than spray-dried CNCs. This approach shows the potential to use Raman spectroscopy to quantify the degree of mixing of CNCs in a thermoplastic matrix.

**Keywords:** Raman Imaging, Cellulose-Nanocrystals, Composites, Thermoplastics

## Introduction

The development of modern composites has triggered an interest in reinforced thermoplastic matrices, since they are potentially re-moldable, low cost and can be formed using mature technology (extrusion, injection molding etc.). Abundantly available, renewable and bio-degradable cellulose based materials are potential candidates for fillers in such matrix materials. Of these, medium aspect ratio cellulose nanocrystals (CNCs) offer potential to reinforce thermoplastics as they could be incorporated into traditional processing routes. One of the main obstacles to the adoption of cellulose fibers in general into mainstream composite materials is their mixing with hydrophobic thermoplastic resins. The hydrophilic nature of CNCs induces the formation of hydrogen bonding between the nanoparticles increasing their tendency to agglomerate in nonpolar matrices. Compatibilizers such as maleic anhydride grafted polyethylene (MAPE)<sup>[1,2]</sup> and polyoxyethylene (PEO)<sup>[3]</sup> have been used to improved chemical compatibility between the matrix and the filler in melt-compounding processes. Characterization of such composites is often focused on the examination of their morphology, physico-chemical and mechanical properties. Analytical methods frequently used to investigate cellulose nanofiber-thermoplastics composites include scanning electron microscopy (SEM)<sup>[1-3]</sup>, differential scanning calorimetry (DSC)<sup>[1,2,4]</sup>, thermogravimetric analysis (TGA)<sup>[1,3,4]</sup>, dynamic mechanical analysis (DMA)<sup>[2,5]</sup>, and mechanical tests<sup>[1,5]</sup>. None of these approaches gives any direct visualization, or enables quantification of a mixing degree of the basic components in the composite. So far confocal Raman microscopy has been used to quantify the efficiency of the processing of thermoplastic composites.<sup>[6,7]</sup>

Recent developments in vibrational spectroscopy methods such as Raman and IR have provided exceptional advantages in delivering detailed structural and molecular information on composite morphology.<sup>[6-11]</sup> New opportunities arise from the progress in vibrational imaging, which combine

the structural and chemical “fingerprint” of spectroscopic analysis with the visualization of optical microscopy. Raman microscopy provides imaging with chemical sensitivity at the submicrometer scale. The combination of Raman spectroscopy with confocal microscopy allows the rejection of out-of-focus Raman scattering generating images with less background, 3D information and improved resolution. Raman imaging has been used to study the distribution of cellulose nanocrystals in a polypropylene matrix composite<sup>[6]</sup>, the compatibility of polymer blends<sup>[7,12]</sup>, biomaterial degradation in vivo<sup>[9]</sup>, the distribution of drug components in hot-melt co-extrudates<sup>[10]</sup>, the characterization of multilayer films<sup>[11]</sup> and the composition of plant cell walls<sup>[13,14]</sup>.

In this communication we show that confocal Raman mapping combined with chemical images and using image analysis provides an evaluation of the spatial distribution of CNCs in high density polyethylene composites. These composites are prepared using maleic anhydride grafted polyethylene by melt-compounding. The conversion of Raman spectra to chemical images provides high contrast and reliability for the analysis. The image analysis approach allows a quantitative assessment of the degree of mixing between components, clearly showing where no intercalation is present.

## **Experimental**

### **Preparation and morphology of composites**

Cellulose nanocrystals (CNCs) (freeze-dried and spray-dried) were purchased from the University of Maine, Process Development Centre; USA. High density polyethylene (Arboblend HDPE; Molecular Weight ( $M_w$ ) = 132839 and Melt Volume Flow Rate (MVR) = 20) was supplied by Tecnaro GmbH, while maleic anhydride grafted polyethylene (A-C 575A, MAPE copolymer) was provided by Honeywell.

The fillers and compatibilizer were blended in a mortar for 2 minutes. Subsequently, the powdered HDPE matrix was added and the components were mixed in a mortar for a further 8 minutes. The mixture was dried in a vacuum oven at a temperature of 60 °C for 24h to remove humidity. HDPE composites containing CNCs were prepared by melt-compounding in a counter rotating twin-screw extruder (HAAKE Rheomex CTW5, Thermo Fisher Scientific) at a temperature of 160 °C. The mixing speed was 70 rpm for 7 min. The composites were extruded in a filament form with a diameter of ~2 mm. Two sets of samples were compounded with CNCs/MAPE/HDPE ratios of 2.5/2.5/95 and 5.0/2.5/92.5 wt%.

The morphology of the cross-section of the composite filament was studied using a HITACHI S3200N SEM-EDS scanning electron microscope operated at an acceleration voltage of 10 kV. Prior to imaging, the composite filament was cryo-microtomed into slices ~20 µm thickness. The cross-sectional area of the cut filament slices was  $\sim 3 \times 10^6 \mu\text{m}^2$ . The slices of composite were fixed on metal stubs using carbon tape and sputter-coated at ~20 mA with a thin layer of gold. The magnifications used for the collection of SEM images were 3000× and 10000×.

### **Raman spectroscopy and Raman imaging**

Raman spectroscopy was performed using a confocal Raman microscope, Alpha300 (WITec) equipped with a thermoelectrically cooled CCD detector (down to – 61 °C). A 532 nm wavelength laser was used for excitation and a 50× objective lens was used for backscattered light collection with a lateral resolution of 388 nm. The spectrometer grating was 600 g/mm, BLZ = 500 nm. Raman spectra of pure CNCs, MAPE and HDPE were recorded using an exposure time of 60 s and two accumulations. Raman mapping measurements were performed on the cross-section of the

composite filament, which was cryo-microtomed prior to measurements. Raman images were recorded in an area of  $50 \times 50 \mu\text{m}^2$  ( $2500 \mu\text{m}^2$ ) with a step size of  $0.2 \mu\text{m}$  in both the  $x$  and  $y$  directions and an exposure time of  $0.1 \text{ s}$  and one accumulation. A total 62500 Raman spectra were recorded for each map. The wavenumber intervals used to calculate images was  $\sim 3.8 \text{ cm}^{-1}$ . The average number of maps per composite was six.

WITec Project Plus software was used to analyze Raman images and to convert them into chemical images. These chemical images were subsequently analyzed using Image-J software to estimate the area in  $\mu\text{m}^2$  and the percentage of the area related to each component of the chemical image. Image-J required a conversion of the chemical maps to a greyscale image, where the white part was referred as the foreground (object) and the black part the background. The extraction of the objects was performed by an automated threshold with the algorithm IsoData. The role of the algorithm was to set one or two (upper and lower) cut-off values separating specific pixel intensities from each other. A thresholded area was measured taking into account parameters such as 'Area', 'Area Fraction' and 'Limit to Threshold'.

## Results and discussion

### Morphology of composites

Figure 1 depicts the representative SEM images of cross-section areas of CNCs-HDPE composites, where freeze-dried CNCs are labelled as CNCs(FR) and spray-dried CNCs as CNCs(SP). The surfaces of the cross-sections of the composites are smooth with distinguishable cellulose nanocrystals aggregates.

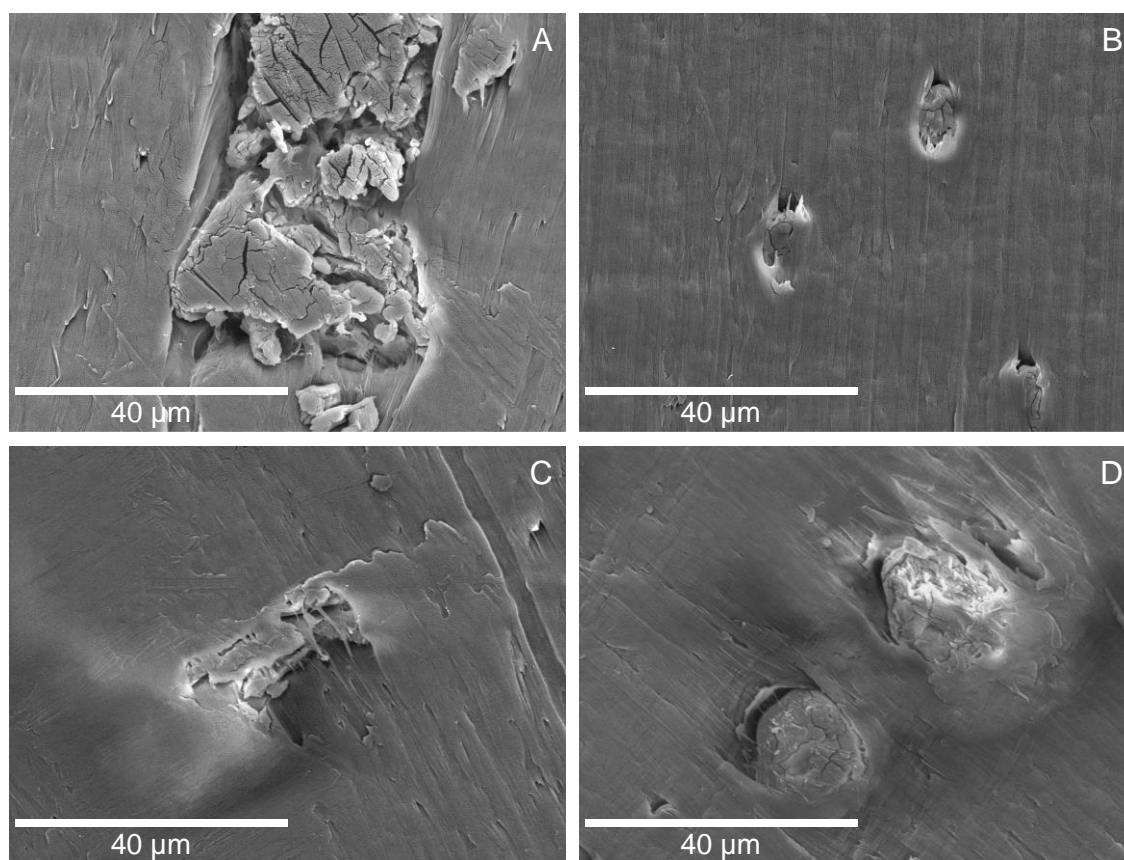


**Figure 1.** Typical SEM images of cryo-microtomed CNCs-HDPE composites at a magnification of 3000 $\times$ : (A) 2.5% CNCs(FR)-HDPE, (B) 2.5% CNCs(SP)-HDPE, (C) 5.0% CNCs(FR)-HDPE, (D) 5.0% CNCs(SP)-HDPE.

The morphology of CNCs aggregates is determined by the drying process of cellulose source. The freeze-dry CNCs look and feel like cotton wool, while the spray-dried resemble sand grains (Figure S1 - Supplementary Materials). Freeze-dried CNCs form irregular shapes (Figure 1A and C) whereas spray dried CNCs form spherical-like shapes (Figure 1B and D). Additionally, there are visible voids in the HDPE matrix proximal to the aggregates. These voids may derive from poor interfacial adhesion between CNCs and HDPE.<sup>[4]</sup> They may also originate from the cryo-microtome cutting process, since the location of the voids is consistent with the direction of the cut visible on the surface of HDPE matrices, Figure 1. The images at a higher magnification reveal the presence of broken filamentous polymer between CNCs aggregates and the HDPE matrix, confirming that there is some interaction between these components (Figure S2 – Supplementary Materials).

SEM images do not give any indication of the degree of mixing between CNCs in the HDPE matrix; nor do optical microscope images (Figure S1 - Supporting Information). To obtain this information we used a Raman spectroscopic method, which gives much more detailed information close to the interface between CNCs and the HDPE polymer.

### **Raman imaging**

Figure 2 shows typical Raman spectra of the individual components of the composites; namely CNCs, MAPE and HDPE. Characteristic Raman bands are used for distinguishing these components in Raman images. Raman spectra of freeze-dried and spray-dried CNCs exhibit two features characteristic for cellulose and absent in HDPE (Figure 2A); namely the band centered at  $\sim 1097\text{ cm}^{-1}$  corresponding to the C–O ring stretching modes and the  $\beta$ -1,4 glycosidic linkage (C–O–C) stretching modes between the glucose rings of the cellulose chains.<sup>[15-17]</sup> Additional verification of the presence of CNCs results from the bands found at 250-600  $\text{cm}^{-1}$  assigned to skeletal-bending modes involving the CCC, COC, OCC and skeletal stretching modes of CC and CO.<sup>[17]</sup>

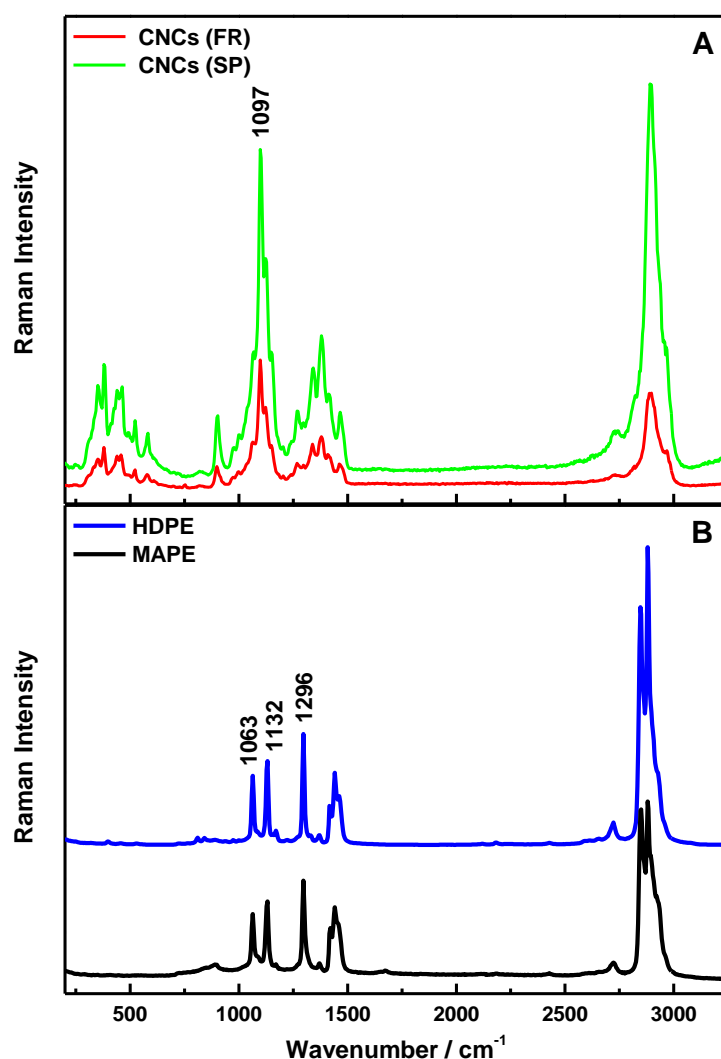


**Figure 2.** Typical Raman spectra of pure composite components: (A) freeze-dried CNCs (CNCs(FR)) and spray-dried CNCs (CNCs(SP)) and (B) maleic anhydride grafted polyethylene (MAPE) and high density polyethylene (HDPE)

The Raman spectrum for maleic anhydride grafted polyethylene exhibits bands unique bands; for example a narrow band at  $\sim 1296 \text{ cm}^{-1}$  corresponding to  $\text{CH}_2$  twisting modes in the crystalline phase.<sup>[18,19]</sup> Furthermore, Raman bands located at  $\sim 1063 \text{ cm}^{-1}$  and  $\sim 1132 \text{ cm}^{-1}$  assigned to C-C stretching modes in crystalline and anisotropic phases of polyethylene are used in the analysis.<sup>[18,19]</sup>

The production of composites with enhanced mechanical properties requires good mixing and/or dispersion of fillers in the matrix and strong interfacial adhesion between both phases. The compatibility between cellulose (hydrophilic) and polyethylene (hydrophobic) is increased by addition of maleic anhydride grafted polyethylene.<sup>[20]</sup> The interaction of the maleic anhydride groups ( $-\text{COOH}$  and  $-\text{C}=\text{O}$ ) and the hydroxyl group ( $-\text{OH}$ ) of cellulose takes place via an esterification reaction and/or hydrogen bonding.<sup>[20]</sup> The ratio of ester linkages to hydrogen bonds depends on the ratio of cyclic anhydride to dicarboxylic acid forms in MAPE.<sup>[20]</sup> The degree of mixing of cellulose in HDPE and the interfacial region where this intimate interaction between MAPE and CNCs takes place can be distinguished using Raman mapping. Figures 3 and 4 illustrate Raman images of CNCs-HDPE composites.

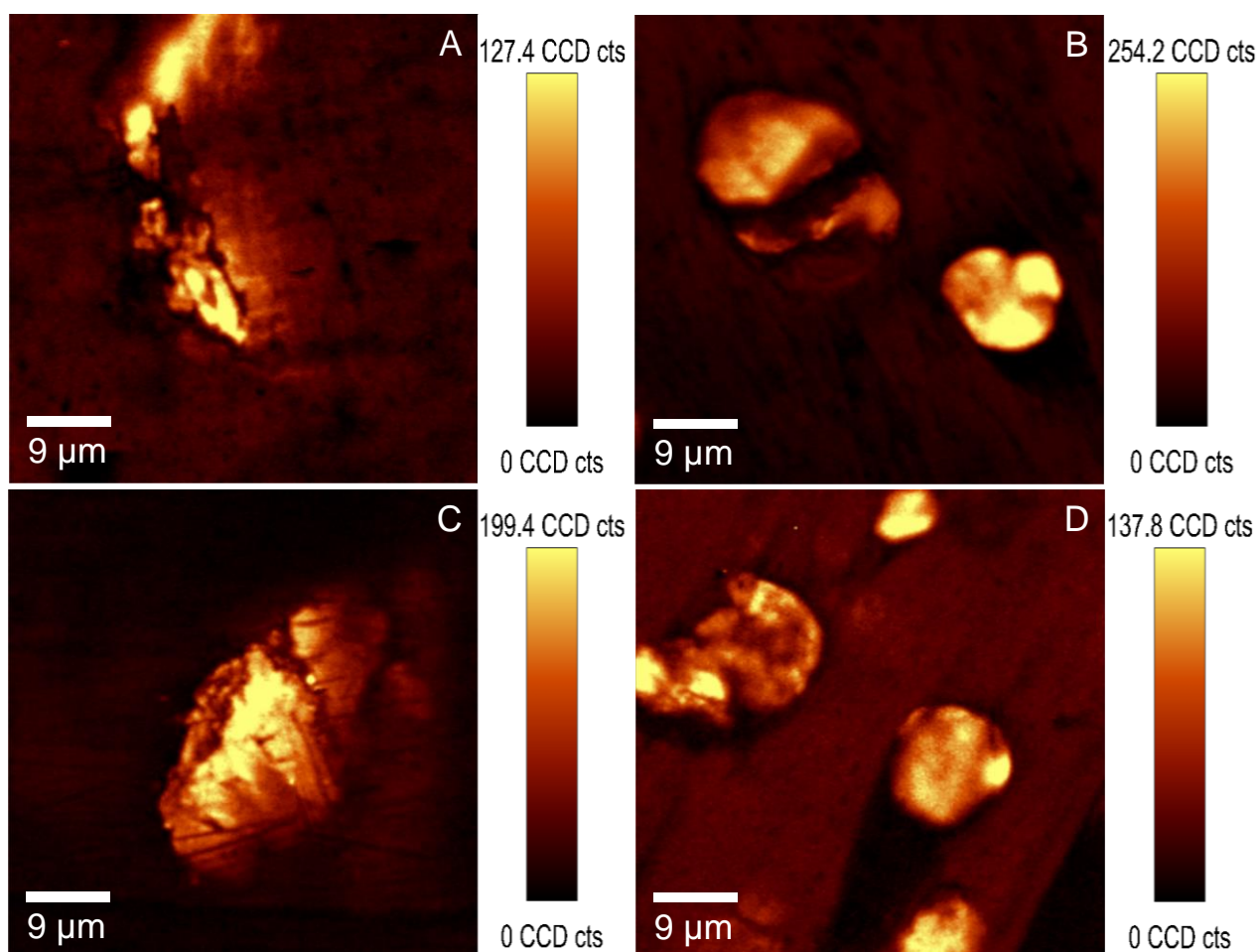


**Figure 3.** Typical Raman images of CNCs-HDPE composites depicting the intensity of a Raman band located at  $\sim 1097\text{ cm}^{-1}$ : (A) 2.5% CNCs(FR)-HDPE, (B) 2.5% CNCs(SP)-HDPE, (C) 5.0% CNCs(FR)-HDPE, (D) 5.0% CNCs(SP)-HDPE.



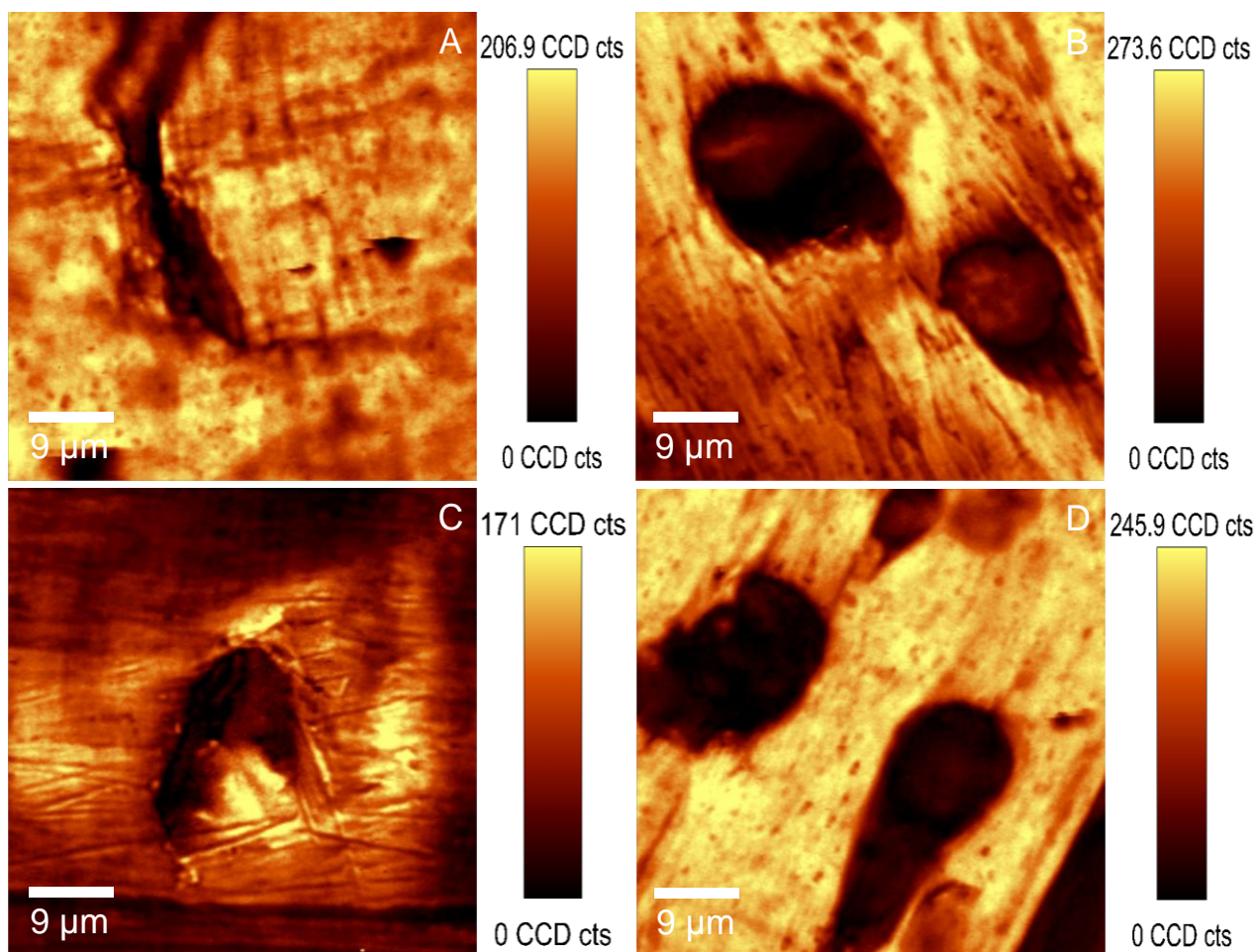


**Figure 4.** Typical Raman images of CNCs-HDPE composites depicting the intensity of a Raman band located at  $\sim 1296\text{ cm}^{-1}$ : (A) 2.5% CNCs(FR)-HDPE, (B) 2.5% CNCs(SP)-HDPE, (C) 5.0% CNCs(FR)-HDPE, (D) 5.0% CNCs(SP)-HDPE.

The bright areas observed in Figure 3 represent regions where the intensity of the Raman band centered at  $\sim 1097\text{ cm}^{-1}$  is strong, confirming the appearance of CNCs in the mapped area. Figure 4 represents images of the intensity of the Raman band located at  $\sim 1296\text{ cm}^{-1}$  corresponding to  $\text{CH}_2$  twisting modes in polyethylene. In both Figures 3 and 4, a brown color indicates the area, where the selected Raman bands do not appear or their intensity is significantly low, while a bright yellow color corresponds to the highest intensity of these bands. CNCs appear to form ‘islands’ in the polyethylene matrix, indicating considerable aggregation, which is consistent with the scanning microscopy images. The shapes of these ‘islands’ are irregular for freeze-dried CNCs (Figure 3A and C) and more spherical for spray-dried CNCs (Figure 3B and D). Raman images reveal that the fillers (CNCs) are mixed with the matrix (HDPE) rather than dispersed in the volume of polyethylene. Additionally, the intensity of the selected Raman bands at the images reflects the surface morphology for the specific component of the composite. Images depicting the intensity of Raman band centered at  $\sim 1296\text{ cm}^{-1}$  show the surface features associated with a direction of the cut of the slices. A lower intensity of the band at  $\sim 1296\text{ cm}^{-1}$  (deep brown color) corresponds to the presence of the aggregates of CNCs and voids.

The degree of interaction between CNCs and HDPE and the degree of agglomeration of the cellulose is evaluated from the chemical images extracted from Raman images. Figure 5 shows chemical images of CNCs-HDPE composites presented in Figures 3 and 4.



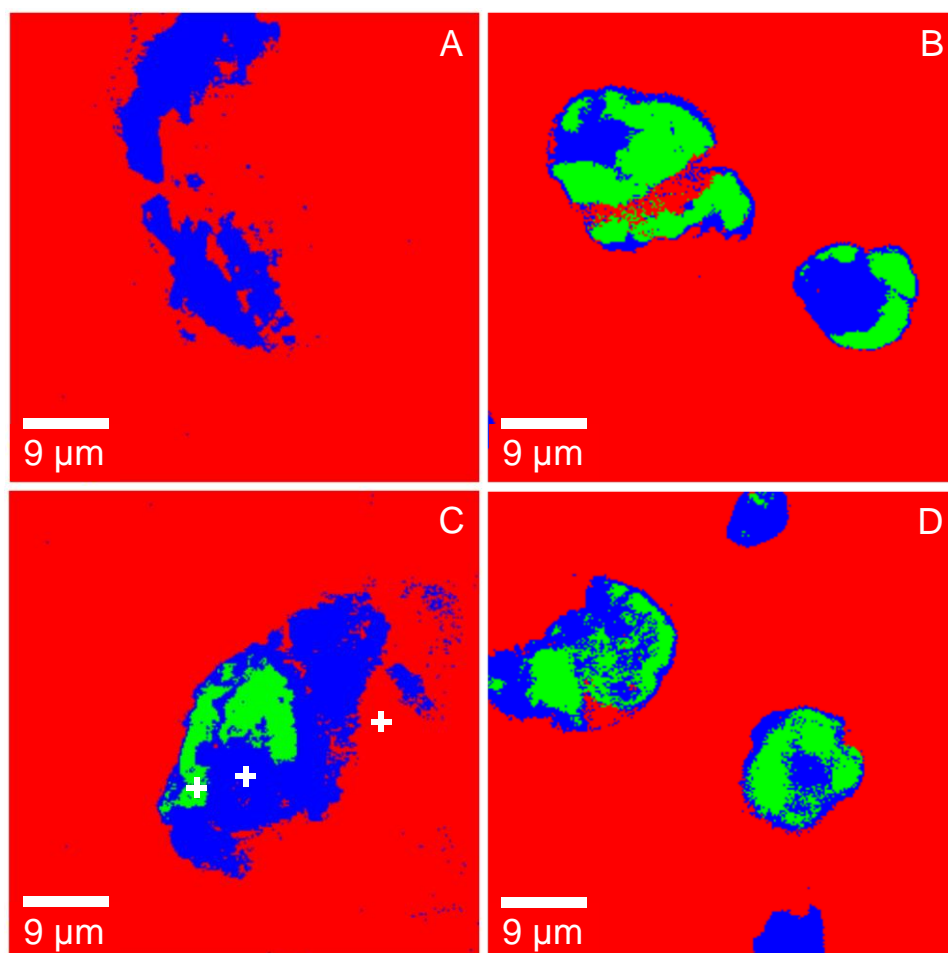


**Figure 5.** Chemical images of CNCs-HDPE composites depicting the chemical composition of a mapped cross-section: (A) 2.5% CNCs(FR)-HDPE, (B) 2.5% CNCs(SP)-HDPE, (C) 5.0% CNCs(FR)-HDPE, (D) 5.0% CNCs(SP)-HDPE.

Figure 6 displays typical Raman spectra corresponding to each component of composite marked with the white crosses at the chemical image on Figure 5C. The areas assigned to HDPE matrix dominate the chemical images (red color on the maps). The Raman spectrum obtained for polyethylene is similar to the raw HDPE used for the melt-compounding process. The areas containing CNCs are represented by both green and blue colors on the chemical maps. They verify once again the tendency of cellulose to aggregate within the HDPE matrix. The Raman spectrum assigned to the green color on the chemical maps matches well the spectra for pure CNCs (Figure 6 and Figure 2A). This indicates the existence of agglomerated CNCs during the compounding process, which is more pronounced for spray-dried CNCs. The region represented by a blue color on the chemical maps appears to be more dominant for freeze-dried CNCs. The Raman spectrum corresponding to an area where mixing has occurred exhibit Raman bands characteristic of both CNCs and HDPE, Figure 6. These areas (colored blue) suggest good mixing of the components. Chemical images therefore allow us to distinguish between regions of close interaction between fillers and between fillers and matrix. This discloses the existence of two antagonistic processes taking place during incorporation of CNCs into a HDPE matrix; the aggregation process and the mixing process.

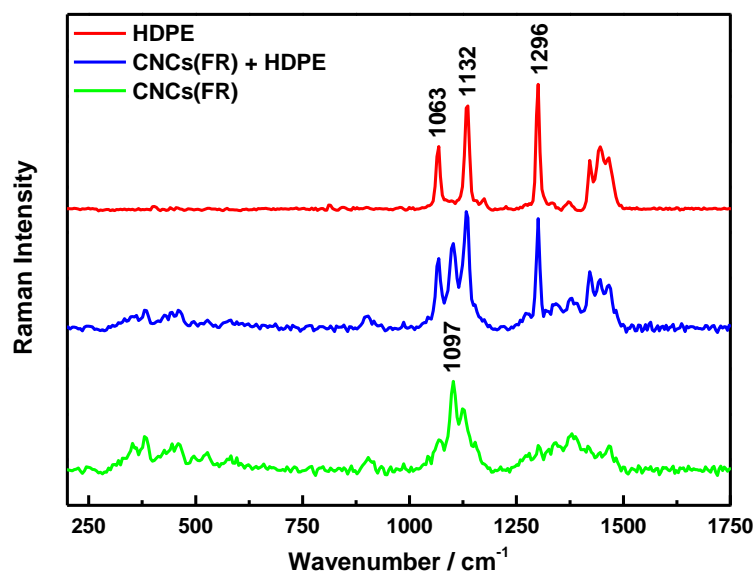


**Figure 6.** Typical Raman spectra of composite components marked with the white crosses at the chemical image of 5.0% CNCs(FR)-HDPE on Figure 5C.

Quantification of mixing of CNCs in polyethylene was performed using Image-J software. Figure S3 (Supplementary Materials) illustrates the grayscale images of the blue areas obtained from the chemical images of CNCs-HDPE composites. The grayscale images consist of a white region which refers to the foreground (object) and a black region corresponding to the background. The conversion of the chemical images to the greyscale combined with a splitting between each color allows the extraction of the objects and a quantification of their respective areas.

Table 1 exhibits the area in  $\mu\text{m}^2$  estimated using Image-J software. The area of each of Raman images is  $2500 \mu\text{m}^2$  in comparison to  $\sim 3 \times 10^6 \mu\text{m}^2$  for the overall cross sectional area of the composite filament. Data obtained from the Raman images are used to quantify the degree of mixing between CNCs and HDPE and the degree of aggregation of CNCs. It is worthwhile noting that the average ratio of agglomerated CNCs to CNCs within an area where mixing with HDPE has occurred (Green area/Blue area), can be used as an indicator of aggregation. These values are much lower for freeze-dried cellulose (CNCs(FR)-HDPE), than for spray-dried cellulose (CNCs(SP)-HDPE). It appears, that the spray dried CNCs have a higher tendency to agglomerate during melt compounding with polyethylene. On the other hand it is possible that, they stay in an intact form of the sand grains initially used for the compounding process, which arise from its industrial drying process. This effect is undesirable in the preparation of good quality nanocomposites. Additionally, the agglomeration of CNCs decreases the observed area corresponding to cellulose, which prevents the use of Raman images and chemical images in an estimation of the stoichiometric ratio of components. Instead, they are only useful for quantifying the degree of mixing between the filler and matrix and to estimate the effectiveness of this process. Freeze-dried CNCs appear to mix to a greater extent with HDPE (Blue area fraction – Table 1) compared to the spray dried material. However, they also occasionally exhibit large agglomerated clusters. Significant standard deviations correlated with the estimated areas indicate variability between evaluated Raman images. These values for Green area/Blue area ratio of fraction are higher for freeze-dried cellulose (CNCs(FR)-HDPE) than for spray-dried cellulose (CNCs(SP)-HDPE). It results from a larger variability of the size of the areas corresponded to the CNCs(FR) ‘islands’.

p-values based on t-tests have been calculated for the ratio of fraction (Green/Blue). These values for the composites with the same CNCs loadings, but different CNC source are 0.08 for 2.5 wt% of CNCs and 0.03 for 5.0 wt% of CNCs. While for the composites with the same CNCs source, but

different CNCs loading are 0.21 for freeze-dried CNCs and 0.23 for spray-dried CNCs. Assuming that an acceptable level of significance is  $p = 0.05$  (95% confidence), most of the compared results are not statistically significant.

The comparison of morphology of the composites' cross-sectional areas with their Raman and chemical images reveals that the drying process of cellulose nanocrystals has an influence on their applicability in composite materials. CNCs(SP)-HDPE composites containing spray-dried CNCs(SP) exhibit fewer voids proximal to the 'islands' of agglomerated nanocrystals. Nevertheless, a compact form of grains lowers their capability to mix with the HDPE matrices comparing with the freeze-dried CNCs(FR). It seems, that a more open form of CNCs(FR) facilitate their interaction with polymer chains of MAPE and HDPE. However, it triggers a significantly higher level of voids. The correlation of these effects is only possible through the use of the Raman imaging approach.

## Conclusions

In conclusion, we have demonstrated that Raman microscopy is a powerful and useful tool for the chemical and spatial quantification of the mixing process of cellulose nanocrystals in thermoplastics. The combination of Raman imaging with image analysis provides rich information regarding the mixing of HDPE with CNCs, and also the agglomeration of the latter in a compounded composite. CNCs are found to form different agglomerated 'islands' within the HDPE dependent on the drying process used for their production. Freeze-dried CNCs appear to exhibit a lower tendency to agglomerate and a better interaction between filler and matrix is also observed. Therefore Raman images provide wider information about the composite quality supported on a detailed chemical quantification and a basic morphological feature of the material.

## Acknowledgments

The authors would like to thank the EU FP7 funding programme for supporting the work under grant agreement no 604168 ([www.newspec.eu](http://www.newspec.eu)). This publication reflects the views only of the author and the European Commission cannot be held responsible for any use which may be made of the information contained therein.

## References

- [1] M. Pöllänen, M. Suvanto, T. T. Pakkanen, *Compos. Sci. Technol.* **2013**, 76, 21.
- [2] P. M. Kosaka, Y. Kawano, H. M. Petri, M. C. A. Fantini, D. F. S. Petri, *J. Appl. Polym. Sci.* **2007**, 103, 402.
- [3] K. Ben Azouz, E. C. Ramires, W. Van den Fonteyne, N. El Kissi, A. Dufresne, *ACS Macro Lett.* **2011**, 1, 236.
- [4] R. Ou, Y. Xie, Q. Wang, S. Sui, M. P. Wolcott, *J. Appl. Polym. Sci.* **2014**, 40331 (1-8).
- [5] J. Li, Z. Song, D. Li, S. Shang, Y. Guo, *Ind. Crop. Prod.* **2014**, 59, 318.
- [6] U. P. Agarwal, R. Sabo, R. S. Reiner, C. M. Clemons, A. W. Rudie, *Appl. Spectrosc.* **2012**, 66, 750.
- [7] S. Huan, W. Lin, H. Sato, H. Yang, J. Jiang, Y. Ozaki, H. Wu, G. Shen, R. Yu, *J. Raman Spectrosc.* **2007**, 38, 260.
- [8] M. D. Schaeberle, H. R. Morris, J. F. Turner II, P. J. Treado, *Anal. Chem.* **1999**, 71, 175A.

- [9] A. A. van Apeldoorn, H.-J. van Manen, J. M. Bezemer, J. D. de Bruijn, C. A. van Blitterswijk, C. Otto, *J. Am. Chem. Soc.* **2004**, *126*, 13226.
- [10] A.-K. Vynckier, L. Dierickx, L. Saerens, J. Voorspoels, Y. Gonnissen, T. De Beer, C. Vervaet, J. P. Remon, *Int. J. Pharm.* **2014**, *464*, 65.
- [11] E. Widjaja, M. Garland, *Mater. Today* **2011**, *14*, 114.
- [12] T. Furukawa, H. Sato, Y. Kita, K. Matsukawa, H. Yamaguchi, S. Ochiai, H. W. Siesler, Y. Ozaki, *Polym. J.* **2006**, *11*, 1127.
- [13] N. Gierlinger, M. Schwanninger, *Plant Physiol.* **2006**, *140*, 1246.
- [14] U. P. Agarwal, *Planta*, **2006**, *224*, 1141.
- [15] N. Gierlinger, M. Schwanninger, A. Reinecke, I. Burgert, *Biomacromolecules* **2006**, *7*, 2077.
- [16] A. E. Lewandowska, C. Soutis, L. Savage, S. J. Eichhorn, *Compos. Sci. Technol.* **2015**, *116*, 50.
- [17] J. H. Wiley, R. H. Atalla, *Carbohydr. Res.* **1987**, *160*, 113.
- [18] H. Sato, M. Shimoyama, T. Kamiya, T. Amari, S. Šašić, T. Ninomiya, H. W. Siesler, Y. Ozaki, *J. Appl. Polym. Sci.* **2002**, *86*, 443.
- [19] S. S. Cherukupalli, A. A. Ogale, *Polym. Eng. Sci.* **2004**, *44*, 1484.
- [20] J. M. Felix, P. Gatenholm, *J. Appl. Polym. Sci.* **1991**, *42*, 609.

Table 1

Average area fraction of the component of chemical maps quantified using Image J software.

Composite	Area fraction			Ratio of fraction	
	Red* [ $\mu\text{m}^2$ ]	Blue* [ $\mu\text{m}^2$ ]	Green* [ $\mu\text{m}^2$ ]	CNCs/HDPE	Green/Blue
2.5% CNCs(FR)-HDPE	$2194 \pm 112$	$238 \pm 98$	$35 \pm 26$	$0.13 \pm 0.06$	$0.16 \pm 0.11$
5.0% CNCs(FR)-HDPE	$2216 \pm 150$	$164 \pm 91$	$60 \pm 67$	$0.12 \pm 0.08$	$0.25 \pm 0.21$
2.5% CNCs(SP)-HDPE	$2265 \pm 85$	$105 \pm 40$	$97 \pm 81$	$0.09 \pm 0.04$	$1.27 \pm 1.48$
5.0% CNCs(SP)-HDPE	$2220 \pm 101$	$148 \pm 54$	$100 \pm 66$	$0.11 \pm 0.05$	$0.72 \pm 0.43$

\* Red – fraction area corresponding to HDPE; \* Blue – fraction area corresponding to CNCs + HDPE; \* Green - fraction area corresponding to CNCs